Replication-dependent histone biosynthesis is coupled to cell-cycle commitment

Claire Armstrong[a,b] and Sabrina L. Spencer[a,b,1]

[a]Department of Biochemistry, University of Colorado, Boulder, CO 80303; and [b]BioFrontiers Institute, University of Colorado, Boulder, CO 80309

Edited by Philip C. Hanawalt, Stanford University, Stanford, CA, and approved June 18, 2021 (received for review January 6, 2021)

The current model of replication-dependent (RD) histone biosynthesis posits that RD histone gene expression is coupled to DNA replication, occurring only in S phase of the cell cycle once DNA synthesis has begun. However, several key factors in the RD histone biosynthesis pathway are up-regulated by E2F or phosphorylated by CDK2, suggesting these processes may instead begin much earlier, at the point of cell-cycle commitment. In this study, we use both fixed- and live-cell imaging of human cells to address this question, revealing a hybrid model in which RD histone biosynthesis is first initiated in G1, followed by a strong increase in histone production in S phase of the cell cycle. This suggests a mechanism by which cells that have committed to the cell cycle build up an initial small pool of RD histones to be available for the start of DNA replication, before producing most of the necessary histones required in S phase. Thus, a clear distinction exists at completion of mitosis between cells that are born with the intention of proceeding through the cell cycle and replicating their DNA and cells that have chosen to exit the cell cycle and have no immediate need for histone synthesis.

restriction point | replication-dependent histone | NPAT | SLBP | histone locus body

To accommodate DNA replication in S phase of the cell cycle, histone proteins, the building blocks of the nucleosome, must double in number to maintain the proper compaction and organization of genomic DNA. Ensuring the correct cell-cycle timing of histone protein synthesis is vital to cellular health and preventing genomic instability, which can lead to age-related pathologies (1–3). Up-regulation of these cell-cycle–dependent canonical histones, otherwise known as replication-dependent (RD) histones, is thought to be intrinsically linked to S phase entry and initiation of DNA replication (4).

Transcription and translation of RD histone genes is a unique process that requires the coordination of several key factors. The nucleosome consists of four core histones, histone proteins H2A, H2B, H3, and H4, that come together as a 2:2:2:2 octamer, as well as one copy of linker histone protein H1 that binds at the DNA entry and exit sites (5, 6). To provide the histones necessary to stabilize the newly replicated DNA, the cell must produce ∼400 million histone proteins in S phase, which lasts ∼8 h in cultured human cells, to avoid leaving the DNA exposed to genomic instability and deregulation of gene expression (4, 7, 8).

To accomplish this burst of histone production, metazoan RD histone genes are found in evolutionarily conserved clusters containing several copies of each histone gene type, around which a nuclear body can assemble and concentrate the necessary transcription and pre–messenger RNA (mRNA) processing factors (4, 9–12). In humans, this nuclear body, called the histone locus body (HLB), is found at two gene clusters: HIST1, found on chromosome 6, and a smaller cluster HIST2, found on chromosome 1 (13–15). The HLB is dependent on the scaffolding protein, nuclear protein at the ATM locus (NPAT), that seeds formation of the HLB (10, 12, 16–18). Mature RD histone mRNA is not polyadenylated but instead ends in a 3′ stem loop that binds to the stem-loop–binding protein (SLBP), which is necessary for proper processing, nuclear export, and translation (19–23). SLBP is then degraded at the end of S phase to block unnecessary RD histone production once DNA replication is complete (24–27).

Historically, studies have shown that RD histone biosynthesis is linked to DNA replication, beginning at the start of S phase and continuing until the S/G2 boundary (28–30). However, these studies often relied on bulk analysis of synchronized cells—methods which obscure cell-to-cell heterogeneity and disrupt the natural timing of cell-cycle events—with only a few studies suggesting the presence of RD histone mRNA in early G1 (31–34), making it worthwhile to revisit the RD histone biosynthesis pathway with updated cell-cycle tools. Moreover, recent discoveries about the timing of cell-cycle commitment and the link between several key factors of RD histone biosynthesis and the point of cell-cycle commitment suggest that RD histone up-regulation may be coupled to cell-cycle commitment (29, 35–40).

The point at which cells commit to completing their current cell cycle is defined as the restriction point (41–43) and in recent cell-cycle models is viewed as marking the start of G1 phase of the cell cycle (44, 45). The restriction point is followed several hours later by the point at which cells commit to initiating DNA replication, shortly before S phase entry, defined by inactivation of the anaphase-promoting complex (APC) (46). Passage through the restriction point begins with phosphorylation of retinoblastoma protein (Rb) by cyclin-dependent kinase 4 and 6 (CDK4/6), causing the release of the cell-cycle master transcription factor E2F, which up-regulates Cyclin E to activate cyclin-dependent kinase 2 (CDK2), leading to hyperphosphorylation of Rb and complete release of E2F (41, 42). E2F1 drives the up-regulation of cell-cycle genes, including two key RD histone biosynthesis factors, NPAT and SLBP (35). NPAT localization to the HLB, as well as phosphorylation of NPAT by Cyclin E/CDK2, are required for

Significance

Current thinking limits replication-dependent (RD) histone biosynthesis to S phase of the cell cycle, with histone production initiated concomitantly with DNA replication. This work examines the cell-cycle timing of RD histone biosynthesis in single human cells and shows that while there is indeed a burst of RD histone production in S phase, RD histone production actually begins earlier in G1, at the point of cell-cycle commitment. These results demonstrate that cells born committed to the subsequent cell cycle build up a small pool of histones before initiating DNA replication, thereby safeguarding against a loss of genome integrity, and are distinct from cells that have exited the cell cycle and do not require histone synthesis until cell-cycle reentry.

Author contributions: C.A. designed research; C.A. performed research; C.A. analyzed data; S.L.S. conceived of the project; and C.A. and S.L.S. wrote the paper.

The authors declare no competing interest.

This article is a PNAS Direct Submission.

[1]To whom correspondence may be addressed. Email: sabrina.spencer@colorado.edu.

This article contains supporting information online at https://www.pnas.org/lookup/suppl/doi:10.1073/pnas.2100178118/-/DCSupplemental.

Published July 29, 2021.

RD histone gene expression (29, 35–40). The presence of NPAT and SLBP allows for the recruitment of necessary factors to the HLB, transcription of RD histone mRNA, and processing and translation of that mRNA (Fig. 1*A*).

Recent work in the cell-cycle field has shown that a majority of naturally cycling cells are born committed to the cell cycle, with residual and increasing CDK2 activity and hyperphosphorylated Rb (designated "CDK2^{inc} cells"), while a subset of cells enters a transient quiescence (designated "CDK2^{low} cells") (44, 45). Thus, in the CDK2^{inc} cells born committed to the cell cycle, RD histone biosynthesis could hypothetically begin upon completion of mitosis due to the presence of residual CDK2 activity and liberated E2F (Model 2, Fig. 1*B*), rather than be linked to the start of DNA replication (Model 1, Fig. 1*B*) when observed in asynchronously cycling single cells.

A fresh evaluation of RD histone biosynthesis relative to DNA replication is therefore warranted to better understand when and how cells born committed to the cell cycle prepare for S phase in order to minimize the risk of insufficient histone production in early S phase while also avoiding premature production of 400 million histone proteins.

In this study, we examine several stages of the RD histone biosynthesis pathway at a single-cell level in a variety of non-transformed human cells. We find that the RD histone biosynthesis machinery and histone mRNA are up-regulated prior to S phase entry in cells born committed to the cell cycle (CDK2^{inc} cells) relative to cells born into a transient quiescence (CDK2^{low} cells), challenging the longstanding idea that RD histone biosynthesis begins at the start of S phase. However, we also confirm a further burst of histone biosynthesis at the start of S phase. We conclude that the most appropriate model for histone biosynthesis is a hybrid model, wherein synthesis of histone protein is initiated at the point of cell-cycle commitment prior to the onset of S phase, followed by a substantial increase in the rate of histone synthesis at the point of S phase entry.

Results

Histone Biosynthesis Is Initiated in G1 before S Phase Entry. We first analyzed the expression of RD histone genes in our previously published RNA sequencing dataset of newly born CDK2^{inc} versus CDK2^{low} cells and found significant down-regulation of RD histone mRNA in newly born CDK2^{low} cells relative to newly born CDK2^{inc} cells (Fig. 1*C*), consistent with NPAT being a CDK2 substrate and E2F target gene (36, 47). To test whether RD histone biosynthesis is in fact initiated at the point of cell-cycle commitment rather than the start of S phase, we examined the levels of several RD histone biosynthesis factors across the cell cycle in MCF10A mammary epithelial cells, RPE-hTERT retinal epithelial cells, and Hs68 primary neonatal foreskin fibroblasts.

Asynchronously growing cells were fixed and stained for DNA content, phospho-Rb (to indicate cell-cycle commitment), and EdU (to mark cells in S phase). Multiplexing these biomarkers allowed individual cells to then be classified into cell-cycle phases using cutoffs (*SI Appendix*, Fig. S1) for DNA content, hyper- or hypophosphorylated Rb, and EdU positive or negative, as done previously (Fig. 2*A*) (48). Cell-cycle phases are defined as: G0, cells that have exited the cell cycle (i.e., CDK2^{low} cells; 2N DNA content, hypo-pRb, EdU^{-}), G1, cells that have crossed the restriction point (2N DNA content, hyper-pRb, EdU^{-}), S, where cells synthesize a copy of their DNA (hyper-pRb, EdU^{+} cells), and G2/M, cells completing interphase and entering mitosis (4N DNA content, hyper-pRb, EdU^{-}).

In addition to cell-cycle phase markers, cells were stained for either NPAT or SLBP by immunofluorescence (IF) (validated by small interfering RNA (siRNA) knockdown, *SI Appendix*, Fig. S2) or for H1.1, H3.1, or H4.2 histone mRNA by RNA fluorescence

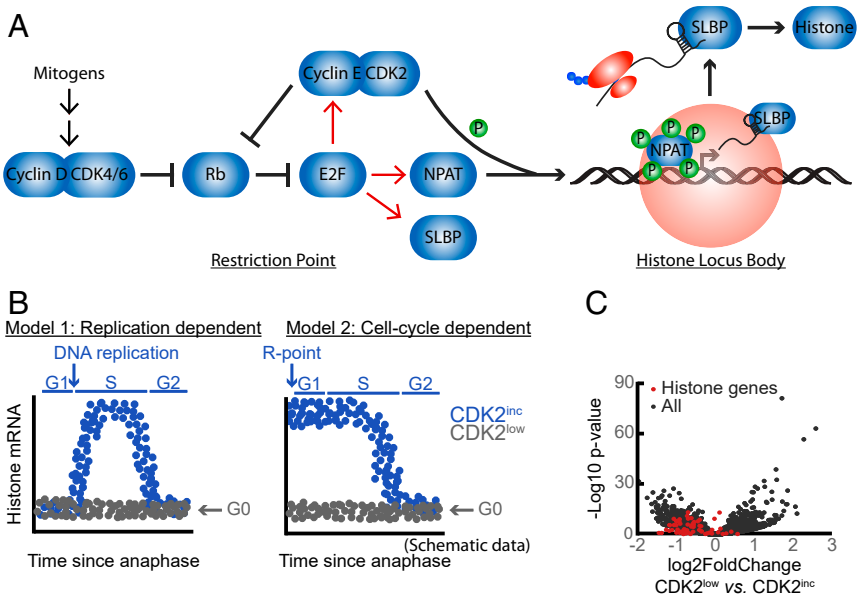

Fig. 1. Connection of RD histone biosynthesis to cell-cycle progression. (*A*) Schematic of the influence of cell-cycle entry on RD histone biosynthesis. Cells in the presence of mitogens will up-regulate Cyclin D/CDK4/CDK6 activity, leading to an initial phosphorylation of Rb, release of E2F, and up-regulation of Cyclin E/CDK2 that will further phosphorylate Rb and push cells through the restriction point (the point of cell-cycle commitment). Liberated E2F causes transcriptional up-regulation (red arrows) of two key factors in RD histone mRNA biosynthesis, NPAT and SLBP, responsible for RD histone mRNA transcription and stability, respectively. CDK2/Cyclin E also phosphorylates NPAT to promote the activation of RD histone transcription. (*B*) Two hypothetical models of RD histone biosynthesis during cell-cycle progression. The canonical model of RD histone biosynthesis has histone production solely coupled to DNA replication in S phase. An alternative model is that in cells born committed to the cell cycle (CDK2^{inc} cells), RD histone production is already high at birth. (*C*) Log2 fold change of RD histone mRNA (red) in CDK2^{low} versus CDK2^{inc} cells, versus all mRNAs measured (black); RNA sequencing data obtained from ref. 47. With only a twofold down-regulation of RD histone mRNAs in CDK2^{low} versus CDK2^{inc} cells, these data do not support either model presented in *B*, but rather imply an intermediate model.

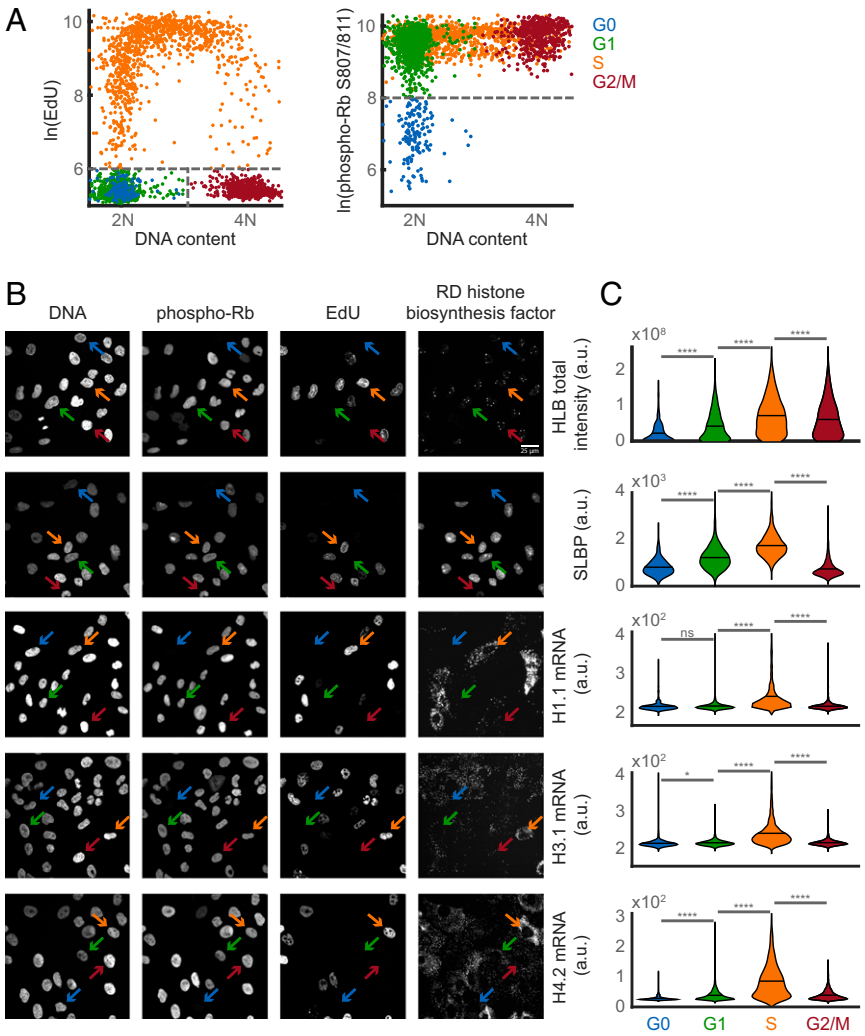

Fig. 2. RD histone genes and synthesis factors are up-regulated in G1 versus G0 MCF10A cells. (*A*) Scatter plot of EdU versus DNA content and phospho-Rb versus DNA content used to define G0 (blue, 5% of cells), G1 (green, 37% of cells), S (orange, 38% of cells), and G2/M (red, 20% of cells). (*B*) Representative images of cells stained with Hoechst to measure DNA content, phospho-Rb S807/811 or S780, and EdU, along with either NPAT, SLBP, or H1.1 (HIST1H1A), H3.1 (HIST1H3A) or H4.2 (HIST2H4A) mRNA. Arrows indicate example cells of each cell-cycle phase; G0 (blue), G1 (green), S (orange), and G2/M (red). Cutoffs for cell-cycle phases can be found in *SI Appendix*, Fig. S1. (*C*) Violin plots by cell-cycle phase of whole-cell median intensity for H1.1, H3.1, and H4.2 mRNA, HLB total intensity (defined in *Materials and Methods*), and median nuclear intensity for SLBP. Axes were determined by maximum and minimum signal for each protein and mRNA. Cell counts and *P* values from two-sample Student's *t* test for each group can be found in *SI Appendix*. *P* values are indicated as $****P \leq 0.0001$, $**P \leq 0.01$, $*P \leq 0.05$, and ns, $P > 0.05$.

in situ hybridization (FISH) (Fig. 2*B*). Histone mRNA probes likely detect all mRNA of each core histone type given the high level of identity between gene copies (13, 14). While several of the histone synthesis factors have been previously described as being up-regulated only in S phase of the cell cycle (49), we observed that H1.1, H3.1, and H4.2 mRNAs are, for the most part, subtly but significantly up-regulated in newly born $CDK2^{inc}$ (G1) versus $CDK2^{low}$ (G0) MCF10A cells (Fig. 2*C*). Histone mRNA expression peaked in S phase and returned to a low level in G2/M (Fig. 2*C*). HLB total intensity also increased from G0 to G1 and G1 to S phase (Fig. 2*C*). Given that Cyclin E begins to rise by 2 h after anaphase in $CDK2^{inc}$ cells (48), it is likely that NPAT is phosphorylated in cells that have crossed the restriction point and therefore that reassembly of the HLB after mitosis is the step required for NPAT "activation" and RD histone gene expression. HLB total intensity decreased slightly in G2/M cells, but the HLB did not fully dissipate, indicating that the HLB may remain stable following the end of S phase until it is disassembled in mitosis (50). SLBP levels increased from G0 to G1 and again from G1 to S phase before experiencing a sharp decrease in G2/M, as would be expected with the degradation of SLBP at the S/G2 boundary (Fig. 2*C*) (49). Similar results were observed in RPE-hTERT (*SI Appendix*, Fig. S3) and Hs68 (*SI Appendix*, Fig. S4) cells, albeit with smaller differences between G0 and G1 in histone mRNA levels, likely due to weaker histone RNA FISH signal in these cells. We conclude that while RD histone protein production peaks in S phase, it is already initiated in G1 phase of the cell cycle.

Two-Tiered Up-Regulation of Histone Biosynthesis. To understand the timing of RD histone up-regulation with fine-grained temporal resolution, we utilized a previously published method to map the EdU and mRNA or protein levels of various RD histone factors to each cell's cell-cycle history (44, 47, 48).

We transduced MCF10A and RPE-hTERT cells with fluorescent histone 2B (H2B) as a nuclear marker, as well as a fluorescent fragment of DNA helicase B (DHB) as a sensor of CDK2 activity (Fig. 3*A*) (45, 51). CDK2 activity was monitored as the cytoplasmic to nuclear ratio of DHB, and cell-cycle progression

was tracked via timelapse imaging (Fig. 3*A*) followed by staining for RD histone biosynthesis factors and EdU incorporation. Cells were aligned to the time of anaphase and categorized as either $CDK2^{inc}$ or $CDK2^{low}$ (*Materials and Methods*). $CDK2^{inc}$ cells were then further categorized as G1 (2N DNA content, EdU^{-}), S (EdU^{+}), or G2 (4N DNA content, EdU^{-}) (*SI Appendix*, Fig. S5).

In MCF10A and RPE-hTERT, total HLB intensity in G1 cells is elevated compared to G0 cells, albeit not significantly so (Fig. 3 *B–C*). Total HLB intensity rises steadily through S phase, before gradually declining throughout the duration of G2 and mitosis (Fig. 3 *B–C*) when the HLB fully disassembles (12, 40). This is in contrast to total HLB size, which reflects the formation of the HLB rather than the concentration of NPAT at the HLB, which in G1 versus G0 cells is statistically significantly higher in MCF10A (*SI Appendix*, Fig. S6). SLBP levels in G1 cells are significantly higher than in G0 cells as soon as 2 h into the cell cycle and increase through G1, where they then remain high throughout the duration of S phase, before declining rapidly in G2 cells (Fig. 3 *B–C*).

Histone H1.1, histone H3.1, and histone H4.2 mRNA levels are already divergent in G1 versus G0 cells 2 h after mitosis in MCF10A cells (Fig. 3*B*). Newly born G1 cells have low but elevated levels of histone mRNAs, whereas histone mRNA biosynthesis remains off in G0 cells throughout the time spent out of the cell cycle. Thus, there is a clear distinction between $CDK2^{inc}$ cells that were born with the intention of proceeding through the cell cycle and replicating their DNA and $CDK2^{low}$ cells that have chosen to exit the cell-cycle and have no immediate need for histone synthesis. This distinction grows even larger in S-phase cells as histone mRNA levels continue to rise and peak in early-to-mid S phase before declining (*SI Appendix*, Fig. S7).

Due to the lower levels of histone mRNA FISH signal in RPE-hTERT cells, the difference in signal between G1 and G0 cells following mitosis is less obvious than in MCF10A cells (Fig. 3*C*). For H4.2 mRNA, the difference between G1 and G0 cells is nevertheless statistically significant at the majority of timepoints in G1, as well as S phase, whereas H1.1 and H3.1 only have significantly elevated levels of mRNA in S phase (Fig. 3*C*). Both FISH and IF signals were generally lower in RPE-hTERT cells compared to MCF10A cells (Fig. 3 *B–C*), indicating that histone mRNA levels may be near the detection limit when levels are low as they are in G1 cells.

Peak Histone Biosynthesis Occurs in Early-to-Mid S Phase. Since cells aligned to anaphase will be partially out of alignment by the time they reach S phase, we further probed the timing of RD histone biosynthesis relative to S phase entry using time lapse microscopy of a previously published geminin sensor (52) to align the cells to the start of S phase, followed by mapping of mRNA, protein, and EdU levels back to each cell's cell-cycle history (46). (Fig. 4*A* and *SI Appendix*, Fig. S8; *Materials and Methods*). The geminin sensor is degraded by the APC in G0 and G1 phases and begins rising at the start of S phase (46). In cells aligned to the geminin rise time, EdU levels are already elevated by 0.8 h after the rise of geminin and fall to baseline 6 h later, marking the end of S phase (Fig. 4*B*). Total HLB intensity rises in early-mid S phase, is sustained through late S phase, and persists for about 1.5 h in G2 phase before declining. SLBP levels also rise in early-mid S phase but begin declining sooner in late S phase. Both H1.1 and H3.1 histone mRNA peak in early-to-mid S phase, as soon as 1.5 h after geminin rise, before declining through the remainder of mid- and late-S phase (Fig. 4 *B–C*). H4.2 mRNA levels peak slightly later at 2.2 h after geminin rise before declining in late S phase (Fig. 4 *B–C*). These results are consistent with those from Fig. 3, where cells were aligned to the time of anaphase. Consistent with previous work done in bulk cultures (26), these data suggest that histone mRNA degradation is reflective of the decline in DNA replication more so than it is linked to the loss of SLBP or the localization of NPAT to the HLB (Fig. 4*C*).

Discussion

Based on the results presented herein, neither Model 1 nor Model 2 from Fig. 1*B* is appropriate. Instead, the data support a two-tiered increase in histone mRNA levels, with levels being elevated above baseline in newly born cells committed to the cell cycle, followed by a sharp increase in mRNA levels at the G1/S phase boundary. Data from some previous studies are consistent with this model (31–34), but this result has never been shown at a single-cell level with the temporal resolution presented in this work. We thus propose an alternative model wherein RD histone biosynthesis is coupled to both cell-cycle entry and DNA replication (Fig. 4*D*).

RD histone protein synthesis is a core part of maintaining genomic integrity. Expression of these proteins has long been seen as intrinsically coupled to DNA replication since they are required to stabilize the newly synthesized DNA and have a well-documented increase in expression at the start of S phase (4). Logically, however, this does not appear to be a sound strategy for safeguarding the genome against the risk of underproduction of histones. If cells begin the production of RD histones in tandem with the initiation of DNA synthesis, cells risk leaving newly replicated DNA exposed to potential genomic instability through loss of chromatin organization, as well as vulnerability to replication stress and potential loss of epigenetic information through defects in chromosome segregation (3, 53, 54).

We propose that cells safeguard against this risk by initiating RD histone gene expression at the point of cell-cycle commitment, rather than the point of S phase entry, to build up a small pool of available histones before DNA replication begins. By having a two-tiered expression of RD histone proteins as shown in Fig. 4*D*, newly born $CDK2^{inc}$ cells show clear intent to proceed through DNA replication while also containing the burst of RD histone production to S phase when the production of nucleosomes is needed. By contrast, newly born $CDK2^{low}$ cells have essentially no histone mRNA production and thus show no intent to enter S phase, consistent with their quiescent status. Thus, there is substantial heterogeneity in histone production rates that reflects the intended trajectories of newly born cells.

The proposed two-tiered model of histone production suggests a coupling to the two key events of G1, the restriction point, when cells commit to their current cell cycle, and APC inactivation, when cells proceed to DNA replication. Our data open questions about how RD histone gene expression is regulated beyond the formation of the HLB and expression of SLBP. Other factors may also influence RD histone mRNA levels, including HLB-specific factors like flice-associated huge protein (FLASH) or U7 small nuclear ribonucleoprotein (snRNP) (9, 55–59). How these factors could potentially coordinate the timing of the burst of RD histone gene expression remains unknown.

In summary, our data support a combined model in which RD histone biosynthesis is coupled to both cell-cycle entry and DNA replication. Understanding the dynamics and control of histone expression is essential for understanding the dynamic organization of the genome across metazoans. The buildup of histones well before the start of S phase may be an important step in protecting the cell from DNA damage and preserving genomic integrity.

Materials and Methods

Cell Culture and Maintenance. MCF10A (ATCC CRL-10317) were cultured in Dulbecco's Modified Eagle Medium/Nutrient Mixture F12 (DMEM/F12) supplemented with 5% horse serum, 100 ng/mL cholera toxin, 20 ng/mL epidermal growth factor (EGF), 10 μg/mL insulin, 0.5 μg/mL hydrocortisone, and 100 μg/mL both penicillin and streptomycin. RPE-hTERT (ATCC CRL-4000) were cultured in DMEM/F12 supplemented with 10% Fetal Bovine Serum (FBS), 1× Glutamax, and 100 μg/mL of both penicillin and streptomycin. Hs68 (ATCC CRL-1635) were cultured in DMEM supplemented with 10% FBS and 100 μg/mL of both penicillin and streptomycin. Cells were grown in a humidified incubator at 5% CO_2 and 37 °C. Live-cell imaging of MCF10A and RPE-hTERT cells was done in a phenol-red free version of the growth media (Gibco).

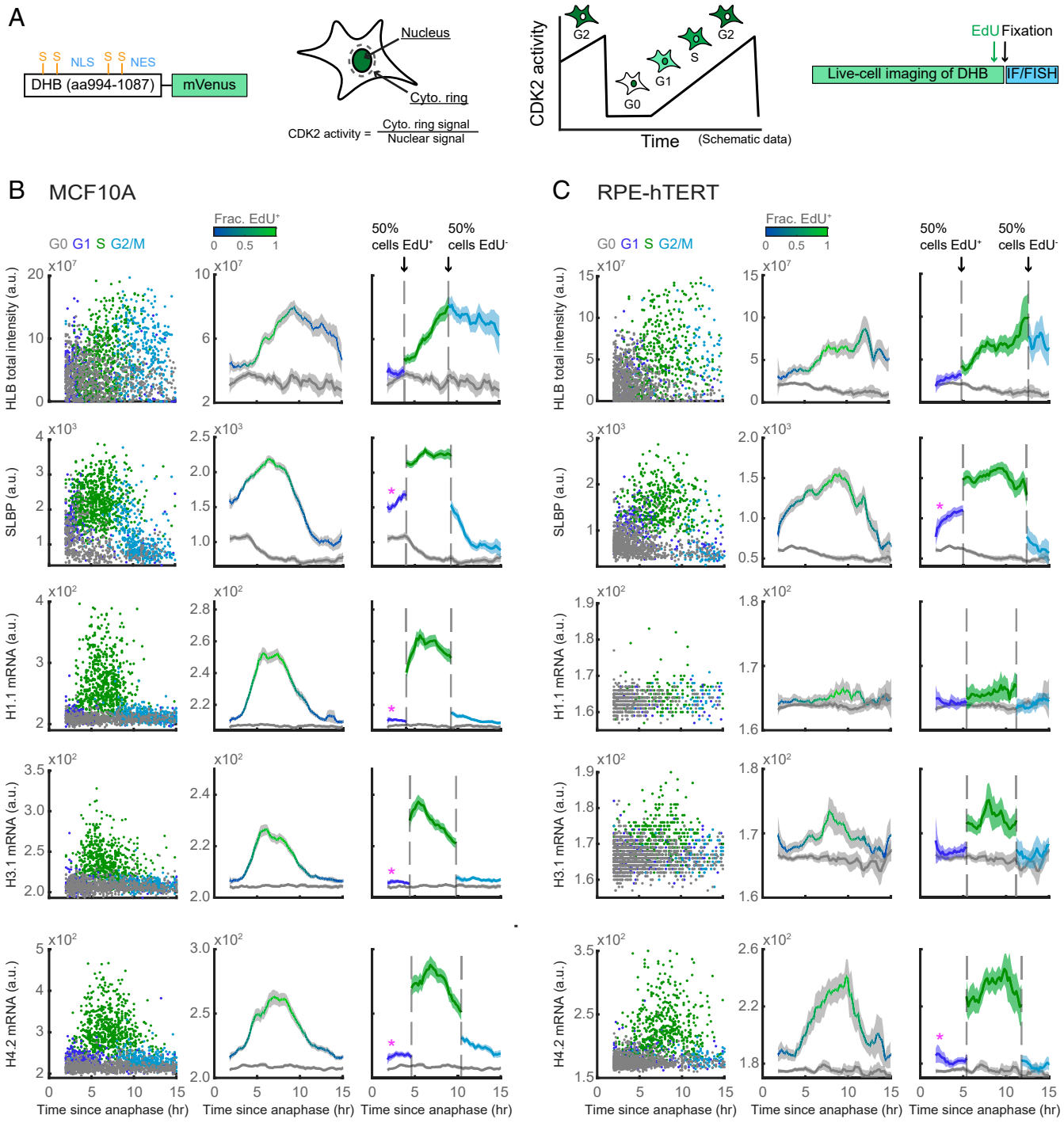

Fig. 3. Dynamics of RD histone biosynthesis during cell-cycle progression. (*A*) Schematic of CDK2 sensor and live-cell tracking (45). (*B–C*) Representative scatter of indicated IF or RNA FISH signal in MCF10A (*B*) or RPE-hTERT (*C*) cells following timelapse imaging of CDK2 activity of an asynchronously cycling population. Cells were treated with EdU in the final 12 min of imaging to further segment cells by cell-cycle phase: G0 ($CDK2^{low}$, EdU^{-}; gray); G1 ($CDK2^{inc}$, EdU^{-}; dark blue); S ($CDK2^{inc}$, EdU^{+}; green); and G2 ($CDK2^{inc}$, EdU^{-}; light blue). Column 1: Raw single-cell data. Column 2: Average protein or mRNA signals and 95% CIs as a function of time since anaphase for populations classified in Column 1 with the fraction of EdU-positive cells at each timepoint indicated by the blue-green gradient. Column 3: Alternative visualization of the data in Column 2 wherein G1 cells (dark blue) are defined as those between anaphase and the timepoint where 50% of cells are EdU positive; S-phase cells (green) as those between the timepoint where 50% of cells are EdU-positive until the timepoint 50% of cells are EdU negative; and G2 cells (light blue) as those from the timepoint where 50% of cells are EdU negative until the end of the cell cycle. Axes were determined by maximum and minimum signal for each protein and mRNA. Non-overlapping shading of 95% confidence intervals (CIs) indicates statistically significant difference as determined by Student's *t* test, with $P < 0.05$, and magenta stars mark signals where at least 90% of timepoints in G1 are statistically significantly higher than in G0 cells. Cell counts can be found in *SI Appendix*.

EdU Incorporation with Immunofluorescence and RNA FISH. Cells were seeded onto 96-well glass-bottom plate (Cellvis Cat. No. P96-1.5H-N) coated with collagen at a 1:50 dilution in water (Advanced BioMatrix, No. 5005) 48 h prior to fixation, at a cell density of 2,000 cells per well for MCF10A, 3,000 cells per well for RPE-hTERT, and 4,500 cells per well for Hs68 cells. EdU was added at 10 μM 15 min before fixation with 4% paraformaldehyde for

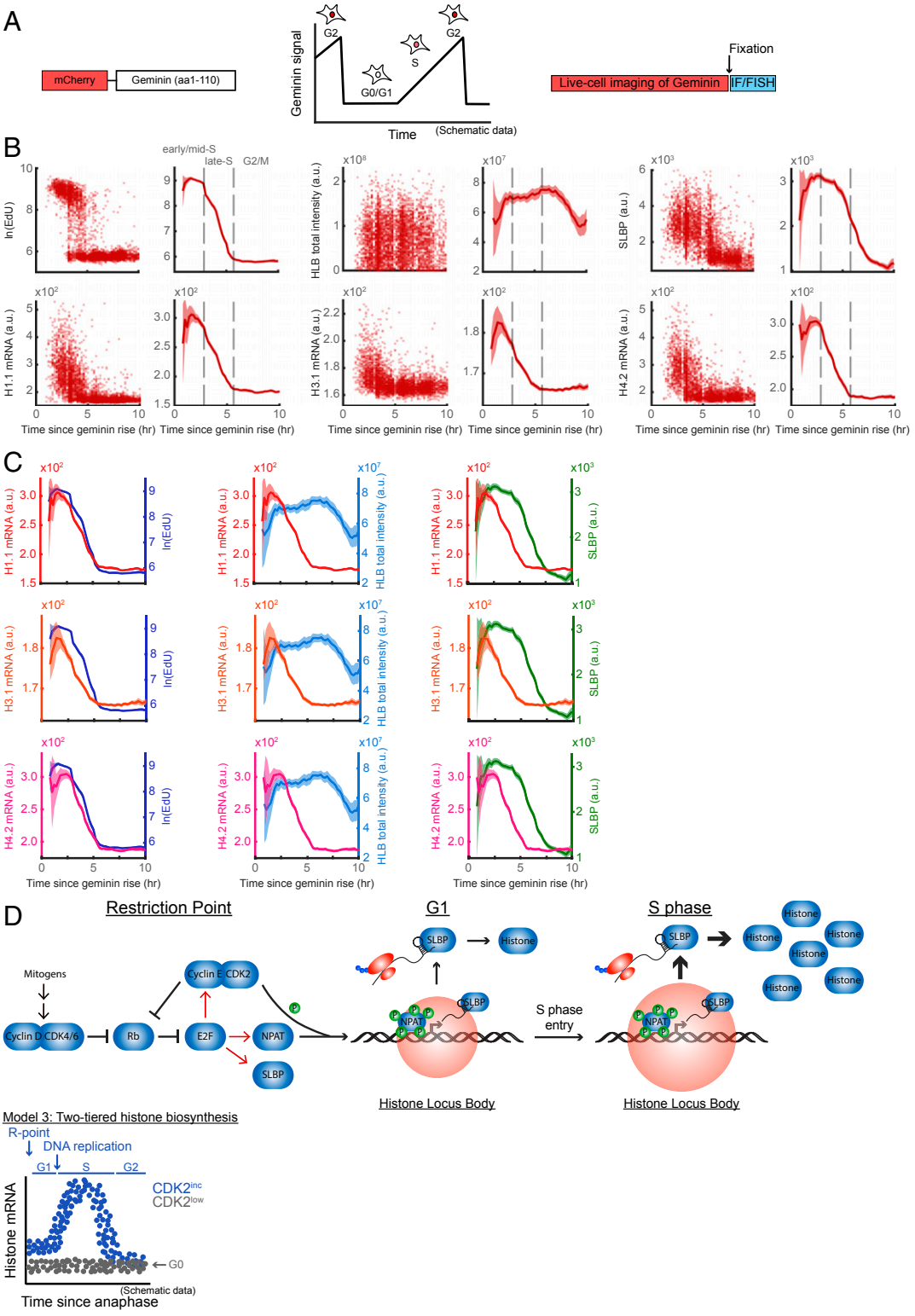

Fig. 4. RD histone biosynthesis relative to S phase entry. (*A*) Schematic of geminin sensor and live-cell tracking (52). (*B*) Scatter of EdU, IF, or RNA FISH signal in MCF10A cells aligned to the rise of geminin following timelapse imaging (*Left* column). Average protein or mRNA signal as well as 95% CIs as shaded bands; EdU incorporation was used to estimate the start and end of late S phase (dashed lines; *Right* column). Axes were determined by maximum and minimum signal for each protein and mRNA. (*C*) Overlay of average and 95% CI for H1.1 (red), H3.1 (orange), and H4.2 (pink) histone mRNA with either EdU (dark blue), HLB intensity (light blue), or SLBP (green) aligned to geminin rise. (*D*) An updated model based on data herein, in which RD histone biosynthesis is coupled to both cell-cycle entry and DNA replication. Cell counts can be found in *SI Appendix*.

15 min. mRNA were visualized according the manufacturer's protocol (ViewRNA ISH Cell Assay Kit, ThermoFisher QVC0001), with mRNA probes hybridized for 4 h at 40 °C. Probes included in this study were ViewRNA Type 6 probes ordered from ThermoFisher, HIST2H4A (VA6-3174283-VC), HIST1H1A (VA6-3172011-VC), and HIST1H3A (VA6-3174263-VC). Wells not stained for mRNA were permeabilized in 0.1% TritonX for 15 min, washed three times with 3% Bovine Serum Albumin (BSA), and processed for EdU visualization as described by the manufacturer's protocol (Invitrogen C10340). Subsequent immunofluorescence was done following standard protocols: cells were blocked for 1 h at 37 °C in 3% BSA, primary antibodies were incubated in 3% BSA overnight at 4 °C, cells were washed three times in PBS, secondary antibodies were incubated at room temperature for 2 h, and cells were washed three times in PBS before being incubated with Hoechst at 1:10,000 at room temperature for 15 min. Imaging was done on a Nikon Ti-E with a 20× 0.45 numerical aperture (NA) objective with the appropriate filter applied. Exposure times were set to 200 ms for DAPI, 200 ms for fluorescein isothiocyanate (FITC), 200 ms for Cy3, and 400 ms for Cy5. Image processing was done as previously described (48, 60). Whole-cell median was quantified as the median pixel value of a cytoplasmic mask, which was deteremined by watershed segmentation and the MATLAB function *regionprops* was used to label the cytoplasm of each cell.

Live-Cell Imaging. Image processing, cell tracking, and cell classification were done as previously described (45, 48, 60), with the tracking code available at https://github.com/scappell/Cell_tracking. In this study, IF, EdU, or FISH signals were matched back to the last frame of the live-cell movie using nearest neighbor screening after jitter correction as previously described (47, 48). Additional information is provided in *SI Appendix*.

Data Availability. All study data are included in the article and/or *SI Appendix*.

ACKNOWLEDGMENTS. We thank Bob Duronio for insights on the project and feedback on the manuscript and members of S.L.S. laboratory for general help, especially Justin Moser and Humza Ashraf for additional feedback on the manuscript. This work was supported by NIH Training Grant T32 GM065103-16 (to C.A.), Pew-Stewart Scholar for Cancer Research Award, an American Cancer Society Research Scholar Grant (Grant RSG-18-008-01), and an NIH Director's New Innovator Award (Award 1DP2CA238330-01) (to S.L.S).

1. Z. Hu *et al*., Nucleosome loss leads to global transcriptional up-regulation and genomic instability during yeast aging. *Genes Dev.* **28**, 396–408 (2014).
2. P. Oberdoerffer, An age of fewer histones. *Nat. Cell Biol.* **12**, 1029–1031 (2010).
3. S. Mendiratta, A. Gatto, G. Almouzni, Histone supply: Multitiered regulation ensures chromatin dynamics throughout the cell cycle. *J. Cell Biol.* **218**, 39–54 (2019).
4. R. J. Duronio, W. F. Marzluff, Coordinating cell cycle-regulated histone gene expression through assembly and function of the Histone Locus Body. *RNA Biol.* **14**, 726–738 (2017).
5. K. Luger, A. W. Mäder, R. K. Richmond, D. F. Sargent, T. J. Richmond, Crystal structure of the nucleosome core particle at 2.8 A resolution. *Nature* **389**, 251–260 (1997).
6. M. Koyama, H. Kurumizaka, Structural diversity of the nucleosome. *J. Biochem.* **163**, 85–95 (2018).
7. A. Maya-Mendoza, P. Olivares-Chauvet, A. Shaw, D. A. Jackson, S phase progression in human cells is dictated by the genetic continuity of DNA foci. *PLoS Genet.* **6**, e1000900 (2010).
8. S. Chari, H. Wilky, J. Govindan, A. A. Amodeo, Histone concentration regulates the cell cycle and transcription in early development. *Development* **146**, dev177402 (2019).
9. B. D. Burch *et al*., Interaction between FLASH and Lsm11 is essential for histone pre-mRNA processing in vivo in Drosophila. *RNA* **17**, 1132–1147 (2011).
10. D. C. Tatomer *et al*., Concentrating pre-mRNA processing factors in the histone locus body facilitates efficient histone mRNA biogenesis. *J. Cell Biol.* **213**, 557–570 (2016).
11. A. E. White *et al*., Drosophila histone locus bodies form by hierarchical recruitment of components. *J. Cell Biol.* **193**, 677–694 (2011).
12. A. E. White, M. E. Leslie, B. R. Calvi, W. F. Marzluff, R. J. Duronio, Developmental and cell cycle regulation of the Drosophila histone locus body. *Mol. Biol. Cell* **18**, 2491–2502 (2007).
13. W. F. Marzluff, P. Gongidi, K. R. Woods, J. Jin, L. J. Maltais, The human and mouse replication-dependent histone genes. *Genomics* **80**, 487–498 (2002).
14. S. Jaeger, S. Barends, R. Giegé, G. Eriani, F. Martin, Expression of metazoan replication-dependent histone genes. *Biochimie* **87**, 827–834 (2005).
15. P. N. Ghule *et al*., The subnuclear organization of histone gene regulatory proteins and 3′ end processing factors of normal somatic and embryonic stem cells is compromised in selected human cancer cell types. *J. Cell. Physiol.* **220**, 129–135 (2009).
16. P. N. Ghule *et al*., Staged assembly of histone gene expression machinery at subnuclear foci in the abbreviated cell cycle of human embryonic stem cells. *Proc. Natl. Acad. Sci. U.S.A.* **105**, 16964–16969 (2008).
17. X. C. Yang *et al*., A conserved interaction that is essential for the biogenesis of histone locus bodies. *J. Biol. Chem.* **289**, 33767–33782 (2014).
18. E. A. Terzo *et al*., Distinct self-interaction domains promote Multi Sex Combs accumulation in and formation of the Drosophila histone locus body. *Mol. Biol. Cell* **26**, 1559–1574 (2015).
19. W. F. Marzluff, K. P. Koreski, Birth and death of histone mRNAs. *Trends Genet.* **33**, 745–759 (2017).
20. R. Thapar, W. F. Marzluff, M. R. Redinbo, Electrostatic contribution of serine phosphorylation to the Drosophila SLBP—histone mRNA complex. *Biochemistry* **43**, 9401–9412 (2004).
21. R. Thapar, G. A. Mueller, W. F. Marzluff, The N-terminal domain of the Drosophila histone mRNA binding protein, SLBP, is intrinsically disordered with nascent helical structure. *Biochemistry* **43**, 9390–9400 (2004).
22. M. L. Whitfield *et al*., Stem-loop binding protein, the protein that binds the 3′ end of histone mRNA, is cell cycle regulated by both translational and posttranslational mechanisms. *Mol. Cell. Biol.* **20**, 4188–4198 (2000).
23. M. Zhang, T. T. Lam, M. Tonelli, W. F. Marzluff, R. Thapar, Interaction of the histone mRNA hairpin with stem-loop binding protein (SLBP) and regulation of the SLBP-RNA complex by phosphorylation and proline isomerization. *Biochemistry* **51**, 3215–3231 (2012).
24. T. E. Mullen, W. F. Marzluff, Degradation of histone mRNA requires oligouridylation followed by decapping and simultaneous degradation of the mRNA both 5′ to 3′ and 3′ to 5′. *Genes Dev.* **22**, 50–65 (2008).
25. K. D. Sullivan, T. E. Mullen, W. F. Marzluff, E. J. Wagner, Knockdown of SLBP results in nuclear retention of histone mRNA. *RNA* **15**, 459–472 (2009).
26. M. M. Koseoglu, L. M. Graves, W. F. Marzluff, Phosphorylation of threonine 61 by cyclin a/Cdk1 triggers degradation of stem-loop binding protein at the end of S phase. *Mol. Cell. Biol.* **28**, 4469–4479 (2008).
27. L. Zheng *et al*., Phosphorylation of stem-loop binding protein (SLBP) on two threonines triggers degradation of SLBP, the sole cell cycle-regulated factor required for regulation of histone mRNA processing, at the end of S phase. *Mol. Cell. Biol.* **23**, 1590–1601 (2003).
28. W. F. Marzluff, E. J. Wagner, R. J. Duronio, Metabolism and regulation of canonical histone mRNAs: Life without a poly(A) tail. *Nat. Rev. Genet.* **9**, 843–854 (2008).
29. J. Zhao, B. Dynlacht, T. Imai, T. Hori, E. Harlow, Expression of NPAT, a novel substrate of cyclin E-CDK2, promotes S-phase entry. *Genes Dev.* **12**, 456–461 (1998).
30. U. Günesdogan, H. Jäckle, A. Herzig, Histone supply regulates S phase timing and cell cycle progression. *eLife* **3**, e02443 (2014).
31. M. E. Harris *et al*., Regulation of histone mRNA in the unperturbed cell cycle: Evidence suggesting control at two posttranscriptional steps. *Mol. Cell. Biol.* **11**, 2416–2424 (1991).
32. J. Abbott, W. F. Marzluff, J. G. Gall, The stem-loop binding protein (SLBP1) is present in coiled bodies of the Xenopus germinal vesicle. *Mol. Biol. Cell* **10**, 487–499 (1999).
33. A. J. DeLisle, R. A. Graves, W. F. Marzluff, L. F. Johnson, Regulation of histone mRNA production and stability in serum-stimulated mouse 3T6 fibroblasts. *Mol. Cell. Biol.* **3**, 1920–1929 (1983).
34. N. Heintz, H. L. Sive, R. G. Roeder, Regulation of human histone gene expression: Kinetics of accumulation and changes in the rate of synthesis and in the half-lives of individual histone mRNAs during the HeLa cell cycle. *Mol. Cell. Biol.* **3**, 539–550 (1983).
35. M. Fischer, P. Grossmann, M. Padi, J. A. DeCaprio, Integration of TP53, DREAM, MMB-FOXM1 and RB-E2F target gene analyses identifies cell cycle gene regulatory networks. *Nucleic Acids Res.* **44**, 6070–6086 (2016).
36. G. Gao *et al*., NPAT expression is regulated by E2F and is essential for cell cycle progression. *Mol. Cell. Biol.* **23**, 2821–2833 (2003).
37. T. Ma *et al*., Cell cycle-regulated phosphorylation of p220(NPAT) by cyclin E/Cdk2 in Cajal bodies promotes histone gene transcription. *Genes Dev.* **14**, 2298–2313 (2000).
38. C. Su *et al*., DNA damage induces downregulation of histone gene expression through the G1 checkpoint pathway. *EMBO J.* **23**, 1133–1143 (2004).
39. J. Zhao *et al*., NPAT links cyclin E-Cdk2 to the regulation of replication-dependent histone gene transcription. *Genes Dev.* **14**, 2283–2297 (2000).
40. W. Hur *et al*., CDK-regulated phase separation seeded by histone genes ensures precise growth and function of histone locus bodies. *Dev. Cell* **54**, 379–394.e6 (2020).
41. T. Zarkowska, S. Mittnacht, Differential phosphorylation of the retinoblastoma protein by G1/S cyclin-dependent kinases. *J. Biol. Chem.* **272**, 12738–12746 (1997).
42. P. W. Hinds *et al*., Regulation of retinoblastoma protein functions by ectopic expression of human cyclins. *Cell* **70**, 993–1006 (1992).
43. A. B. Pardee, A restriction point for control of normal animal cell proliferation. *Proc. Natl. Acad. Sci. U.S.A.* **71**, 1286–1290 (1974).
44. J. Moser, I. Miller, D. Carter, S. L. Spencer, Control of the restriction point by Rb and p21. *Proc. Natl. Acad. Sci. U.S.A.* **115**, E8219–E8227 (2018).
45. S. L. Spencer *et al*., The proliferation-quiescence decision is controlled by a bifurcation in CDK2 activity at mitotic exit. *Cell* **155**, 369–383 (2013).
46. S. D. Cappell, M. Chung, A. Jaimovich, S. L. Spencer, T. Meyer, Irreversible APC(Cdh1) inactivation underlies the point of no return for cell-cycle entry. *Cell* **166**, 167–180 (2016).
47. M. Min, S. L. Spencer, Spontaneously slow-cycling subpopulations of human cells originate from activation of stress-response pathways. *PLoS Biol.* **17**, e3000178 (2019).
48. S. Gookin *et al*., A map of protein dynamics during cell-cycle progression and cell-cycle exit. *PLoS Biol.* **15**, e2003268 (2017).
49. M. M. Koseoglu, J. Dong, W. F. Marzluff, Coordinate regulation of histone mRNA metabolism and DNA replication: Cyclin A/cdk1 is involved in inactivation of histone mRNA metabolism and DNA replication at the end of S phase. *Cell Cycle* **9**, 3857–3863 (2010).
50. J. L. Liu *et al*., The *Drosophila melanogaster* Cajal body. *J. Cell Biol.* **172**, 875–884 (2006).

CELL BIOLOGY

51. D. Yu *et al*., A naturally monomeric infrared fluorescent protein for protein labeling in vivo. *Nat. Methods* **12**, 763–765 (2015).
52. B. T. Bajar *et al*., Fluorescent indicators for simultaneous reporting of all four cell cycle phases. *Nat. Methods* **13**, 993–996 (2016).
53. P. N. Ghule *et al*., Fidelity of histone gene regulation is obligatory for genome replication and stability. *Mol. Cell. Biol.* **34**, 2650–2659 (2014).
54. A. Groth *et al*., Human Asf1 regulates the flow of S phase histones during replicational stress. *Mol. Cell* **17**, 301–311 (2005).
55. I. Sabath *et al*., 3′-End processing of histone pre-mRNAs in Drosophila: U7 snRNP is associated with FLASH and polyadenylation factors. *RNA* **19**, 1726–1744 (2013).
56. A. Skrajna *et al*., U7 snRNP is recruited to histone pre-mRNA in a FLASH-dependent manner by two separate regions of the stem-loop binding protein. *RNA* **23**, 938–951 (2017).
57. X. C. Yang, B. D. Burch, Y. Yan, W. F. Marzluff, Z. Dominski, FLASH, a proapoptotic protein involved in activation of caspase-8, is essential for 3′ end processing of histone pre-mRNAs. *Mol. Cell* **36**, 267–278 (2009).
58. X. C. Yang *et al*., A complex containing the CPSF73 endonuclease and other polyadenylation factors associates with U7 snRNP and is recruited to histone pre-mRNA for 3′-end processing. *Mol. Cell. Biol.* **33**, 28–37 (2013).
59. X. C. Yang *et al*., FLASH is required for the endonucleolytic cleavage of histone pre-mRNAs but is dispensable for the 5′ exonucleolytic degradation of the downstream cleavage product. *Mol. Cell. Biol.* **31**, 1492–1502 (2011).
60. M. Arora, J. Moser, H. Phadke, A. A. Basha, S. L. Spencer, Endogenous replication stress in mother cells leads to quiescence of daughter cells. *Cell Rep.* **19**, 1351–1364 (2017).